Strain-induced perpendicular magnetic anisotropy of ⟨100⟩-oriented Ni-Cu superlattices

R. Naik, A. Poli, D. McKague, A. Lukaszew, and L. E. Wenger
Department of Physics and Astronomy, Wayne State University, Detroit, Michigan 48202
(Received 31 October 1994)

The uniaxial perpendicular and magnetocrystalline anisotropies in strained ⟨100⟩-oriented Ni-Cu superlattices have been determined by in-plane and out-of-plane ferromagnetic resonance and magnetization measurements for varying Ni and Cu thicknesses. X-ray-diffraction patterns of the superlattice structure for these films indicate that the Ni lattice contracts while the Cu lattice dilates along the growth direction. Utilizing the measured strain with known elastic and magnetostriction constants for bulk Ni, the calculated strain-induced magnetoelastic anisotropies due to an inverse magnetostriction are in good *quantitative* agreement with the experimentally determined uniaxial perpendicular anisotropies.

The presence of perpendicular magnetic anisotropy in multilayered films has attracted a great deal of interest in recent times because of the possible technological advances in magnetic and magneto-optical recording[1–4] for increased storage capability. Multilayered films of Co/Pt,[1,2] Co/Pd,[3,4] and Co/Au (Refs. 5 and 6) have shown large positive uniaxial anisotropies when the magnetic layer thickness is reduced to few monolayers. The origin of this anisotropy has been attributed to an interface-induced anisotropy arising from the reduced symmetry of the interface atoms, as pointed out by Néel.[7] There are several other factors such as strain, roughness, and atomic mixing at the interfaces which can strongly influence the interface anisotropy.[8] In epitaxial magnetic multilayers, however, one cannot rule out another important source of magnetic anisotropy; i.e., the magnetoelastic anisotropy due to the coherent strain caused by the lattice mismatch between the adjacent layers.[4,6,9–11]

In a recent study using a ferromagnetic resonance (FMR) technique,[12] we have shown that a 50-Å-thick Ni(100) layer epitaxially grown on a seed layer of Cu(100)/Si(100) substrate is spontaneously magnetized perpendicular to the plane of the film. This observation was attributed to a strain-induced perpendicular magnetic anisotropy arising from the inverse magnetostriction associated with the lattice mismatch between the Ni(100) and Cu(100) interface. For thicker Ni(100) films (100–500 Å), smaller uniaxial perpendicular anisotropy fields were observed which were not large enough to overcome the demagnetizing fields. This effect was partially accounted for by a relaxation of the strains due to the formation of misfit dislocations with increasingly thicker films. In the present paper, we report the results of a systematic magnetic study on strained ⟨100⟩-oriented Ni-Cu superlattices grown on Cu(100)/Si(100) substrates by molecular-beam epitaxy (MBE). The strain in these films as well as the periodicity of the superlattice was determined from out-of-plane x-ray-diffraction (XRD) measurements. By measuring the resonant field of the FMR signal as a function of the angle between the dc magnetic-field direction and a crystallographic direction in the film for both in-plane as well as out-of-plane film orientations, the uniaxial perpendicular and magnetocrystalline anisotropies were determined in order to correlate the effect of strain modulations on the magnetic anisotropies in these films. The uniaxial perpendicular anisotropies observed for these superlattices are found to be solely accounted for by a strain-induced magnetic anisotropy which depends not only on the layer thickness of Ni but also on that of Cu.

The Ni-Cu superlattices were prepared in an ultrahigh vacuum using a molecular-beam epitaxy (MBE) deposition system with a base pressure $<1\times10^{-10}$ Torr. The superlattices were grown on a 450-Å-thick Cu(100) seed layer deposited on Si(100) substrates etched with a 10% hydrofluoric acid solution. Ni and Cu were evaporated from two independent electron-beam evaporators with computer-controlled pneumatic shutters and at deposition rates of ~0.5 Å/s. Further details of the deposition system, the growth of Cu(100) seed layer on hydrogen-terminated Si(100), and the growth of epitaxial Ni(100) layers on Cu(100) layers are described elsewhere.[12,13] Reflection high-energy electron-diffraction (RHEED) patterns were continuously monitored during the deposition to study the quality and structure of the superlattice as well as the original Cu seed layer. Four different superlattices were prepared with Ni layer thicknesses of 30, 45, 60, and 90 Å being alternated with Cu layers of 45 Å thickness. This Cu layer thickness is large enough to avoid any significant magnetic exchange coupling between the Ni layers. The total thickness of Ni in each superlattice was kept at 900 Å. Several other superlattices were grown with similar Ni layer thicknesses but alternated with Cu layer thicknesses of 30–120 Å in order to determine the effect of the Cu thickness on the strain and magnetic anisotropies. All films had a 50-Å Cu cap layer for protection from oxidation.

The FMR data were taken at room temperature using standard magnetic-resonance techniques. The microwave reflection spectrometer operates at a frequency of 12 GHz and employs magnetic-field modulation with phase-sensitive detection so that the detected signal is

0163-1829/95/51(6)/3549(5)/$06.00

proportional to the field derivative of the absorbed power. The dc magnetic field, provided by a 12-inch Varian electromagnet, has a range of 0–13 kG and can be rotated in the horizontal plane through a total angle of 360°. The sample is mounted in a TE_{101} rectangular cavity either on a vertical side wall for out-of-plane measurements or on the bottom wall for in-plane measurements. Typical FMR samples were 4 mm × 4 mm and were aligned along cleavage faces of the Si substrate. Room-temperature magnetic hysteresis loops were measured by using a vibrating sample magnetometer to verify the easy magnetization axis direction. Standard θ-2θ x-ray-diffraction (XRD) scans were performed with Cu $K\alpha$ radiation.

Sharp and elongated spotty RHEED patterns were observed during the growth of all Ni-Cu superlattice films indicating an epitaxial but three-dimensional growth. The full fourfold azimuthal symmetry of the ⟨100⟩ orientation for the Ni-Cu superlattices was clearly observable for all the films. Since both Cu and Ni have bulk face-centered-cubic structures with a lattice mismatch of 2.5%, one can expect a strained, epitaxial superlattice growth. High-angle x-ray-diffraction measurements on all of the thin-film samples confirm ⟨100⟩-oriented growth of the Ni-Cu superlattice ($2\theta \approx 50-52°$) with no trace of the ⟨111⟩ texture ($2\theta \approx 43-45°$). Figure 1(a) shows the XRD scan for a Ni-Cu superlattice with Ni layer thickness of 60 Å and Cu layer of thickness of 45 Å. One observes that the zeroth-order superlattice peak is flanked by higher-order superlattice peaks. In order to interpret the x-ray data quantitatively, the model described by Lamelas, He, and Clarke[14] is utilized. This one-dimensional x-ray-scattering model can include discrete layer thickness fluctuations and interface diffusion in the kinematic approximation. Comparisons of the simulated XRD patterns from this model to the observed peak patterns from the Ni-Cu superlattices indicate a strong dependence upon the lattice spacing modulations and a relative insensitivity to composition modulations, very similar to the observations on Co-Cu superlattices.[14] Figure 1(b) shows the simulated XRD intensities for the above superlattice with Ni(200) and Cu(200) lattice spacings of 1.745 and 1.834 Å, respectively. Without such strain modulations, the superlattice features are not produced as shown in Fig. 1(c) for a simulation with bulk lattice spacings of 1.762 and 1.808 Å for Ni(200) and Cu(200) planes, respectively. The inclusion of layer fluctuations and interlayer diffusion into the simulations just broadens the peak widths and reduces the intensities of the higher-order superlattice peaks. The $d_\perp$ ($=d_{200}$) spacings for both Ni and Cu in these superlattices are determined from the best fit of the simulations to the experimental XRD data (see Table I)

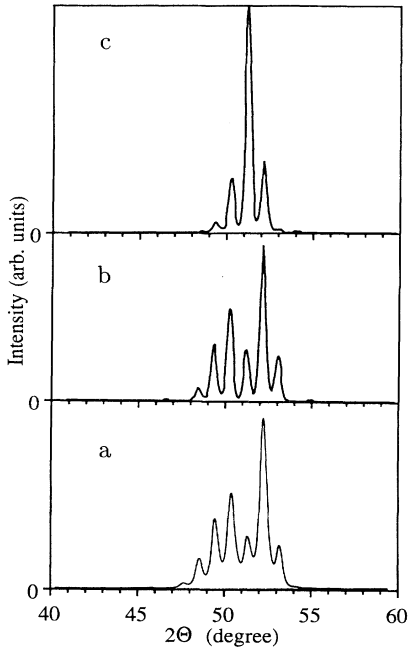

FIG. 1. (a) The high-angle x-ray diffraction pattern for the Ni-Cu superlattice with Ni layer thickness of 60 Å and Cu layer of thickness of 45 Å (film No. 3). Simulations of the XRD intensities for the same superlattice (b) with Ni(200) and Cu(200) lattice spacings of 1.745 and 1.834 Å and (c) bulk lattice spacings of 1.762 and 1.808 Å.

TABLE I. XRD and FMR results for ⟨100⟩-oriented Ni-Cu superlattices.

Film No.	t_{Ni} (Å)	t_{Cu} (Å)	N repeats	Ni d_{200} (Å)	Cu d_{200} (Å)	Ni $(\varepsilon_\perp - \varepsilon_\parallel)$[b]	$4\pi M_{eff}$ (kG)	$2K_1/M_s$ (kG)	[a]H_u (FMR) (kG)	H_u (Calc.) (kG)
1	30	45	30	1.739±0.002	1.830±0.002	−0.0276±0.0024	−1.3±0.2	−0.60±0.05	7.4±0.2	7.2±0.6
2	45	45	20	1.744±0.002	1.832±0.002	−0.0216±0.0024	1.2±0.2	−0.10±0.05	4.9±0.2	5.6±0.6
3	60	45	15	1.745±0.002	1.834±0.002	−0.0203±0.0024	1.3±0.2	−0.30±0.05	4.8±0.2	5.3±0.6
4	90	45	10	1.750±0.002	1.836±0.002	−0.0144±0.0024	2.6±0.2	−0.18±0.05	3.5±0.2	3.7±0.6
5	30	90	10	1.735±0.002	1.825±0.002	−0.0323±0.0024	−2.9±0.2	−0.20±0.05	9.0±0.2	8.4±0.6
6	45	90	10	1.734±0.002	1.823±0.002	−0.0336±0.0024	−3.0±0.2	−0.50±0.05	9.1±0.2	8.7±0.6
7	60	90	10	1.736±0.002	1.822±0.002	−0.0312±0.0024	−2.4±0.2	−0.80±0.05	8.5±0.2	8.1±0.6
8	90	90	10	1.739±0.002	1.822±0.002	−0.0276±0.0024	−1.3±0.2	−0.60±0.05	7.4±0.2	7.2±0.6
9	45	30	10	1.744±0.002	1.832±0.002	−0.0216±0.0024	1.1±0.2	−0.48±0.05	5.0±0.2	5.6±0.6
10	45	60	10	1.739±0.002	1.829±0.002	−0.0276±0.0024	−1.4±0.2	−0.22±0.05	7.5±0.2	7.2±0.6
11	45	120	10	1.734±0.002	1.820±0.002	−0.0336±0.0024	−3.0±0.2	−0.66±0.05	9.1±0.2	8.7±0.6

[a]$H_u = 4\pi M_s - 4\pi M_{eff}$ where $4\pi M_s = 6.08$ kG for bulk Ni.
[b]$\varepsilon_\parallel = -\varepsilon_\perp(1-\nu)/2\nu$ where ν is the Poisson ratio. $\nu = 0.31$ for Ni.

and clearly show that the Ni lattices are contracted while the Cu lattices are dilated along the growth direction. This is consistent with the anticipated results since the lattice mismatch arising from the smaller (200) spacing of Ni should cause an expansion of the Ni lattice in the direction parallel to the film plane and a contraction of the lattice perpendicular to it. This tetragonal distortion amounts to a few percent as reflected by the negative values of $(\varepsilon_\perp - \varepsilon_\parallel)$ for Ni shown in Table I, where $\varepsilon_\perp$ and $\varepsilon_\parallel$ are the perpendicular and parallel strains, respectively. $\varepsilon_\perp = (d_\perp - d_0)/d_0$ and $\varepsilon_\parallel$ are evaluated using the relation $\varepsilon_\parallel = -\varepsilon_\perp(1-\nu)/2\nu$ where d_0 is the undistorted Ni spacing and the Poisson ratio $\nu = 0.31$ for Ni. This tetragonal distortion, $(\varepsilon_\perp - \varepsilon_\parallel)$, is sensitive to not only the Ni layer thickness, but also to the Cu layer thickness.

Both in-plane and out-of-plane FMR data are analyzed by solving energy density expressions under equilibrium and resonance conditions for a $\langle 100 \rangle$-oriented ferromagnetic film.[12] Resonance fields for in-plane FMR measurements on all films exhibit an oscillatory angular dependence with respect to a $\langle 100 \rangle$ crystallographic direction in the film which reflects the fourfold symmetry of the Ni layers. For example, Fig. 2 shows such a dependence for film No. 3. From fits to angular dependence of the experimental resonance data, the effective demagnetization field $4\pi M_{\text{eff}}$ and the cubic anisotropy contribution $2K_1/M_s$ are determined (see Table I) where K_1 is the fourth-order cubic anisotropy constant and M_s is the saturation magnetization. The presence of any perpendicular magnetic anisotropy H_u can be numerically determined from the relationship $H_u = 4\pi M_s - 4\pi M_{\text{eff}}$. Utilizing bulk Ni values of $g = 2.21$ and $4\pi M_s = 6.08$ kG, the calculated values of H_u for all films except films No. 2, 3, 4, and 9 indicate that they are large enough to overcome the demagnetizing field and hence the easy magnetization axis is perpendicular to the plane of the film. For films No. 2, 3, 4, and 9, the easy axis of magnetization lies in the plane of the film. One further notes that the H_u values for these films are consistently smaller than those found for single-layer Ni(100) films of comparable thicknesses on Cu(100)/Si(100) substrates.[12] We attribute this to a decrease in the strain of the Ni layers in the superlattices as compared to the single-layer films. This decrease in strain is clearly indicated from the XRD measurements. In the superlattices, both the Ni and the Cu lattices are coherently strained. We expect an in-plane tensile strain and an associated perpendicular compressive strain in Ni lattice due to its epitaxial growth on the Cu(100) lattice. Indeed all the superlattices show a compressive strain in the Ni layers along the growth direction. On the other hand, Cu lattice shows an expansion of the interplanar spacings along the growth direction suggesting an in-plane compressive strain.

Results for the out-of-plane FMR measurements of the resonance field vs ϕ_H, the angle between the applied magnetic field and the film plane, were carried out on all the samples. The results are presented in Fig. 3 for Ni-Cu films No. 2 (45–45 Å) and No. 6 (45–90 Å). The data for film No. 2 (as well as for Nos. 3, 4, and 9) are characterized by the smallest resonance field occurring at $\phi_H = 0$ and increasing to larger values as the applied magnetic field is rotated away from the plane of the film. This behavior is consistent with an in-plane easy magnetization axis. On the other hand, the data for film No. 6 with the larger Cu layer thickness exhibits an easy magnetization axis perpendicular to the plane of the film as the smallest resonance field occurs at $\phi_H = 90°$ and increases to larger fields as the applied magnetic field is rotated towards the plane of the film. Even though the Ni layer thickness remains the same in both the films, the direction of the easy magnetization axis changes with the increased Cu layer thickness. This change in easy axis direction is directly observable from the magnetization hysteresis loops for applied magnetic fields parallel and perpendicular to the plane of the film as shown in Fig. 4. The ability to saturate the magnetization in smaller fields for the perpendicular direction than the parallel direction indicates the easy axis lies perpendicular to the film plane. Furthermore this change is quantitatively reflected in the parameters used to fit the resonance data as indicated by the solid lines in Fig. 3. The effective demagnetization field $4\pi M_{\text{eff}}$ changes sign for the thicker Cu layer superlattices indicating a change in the easy axis direction as well as a substantial increase in the uniaxial

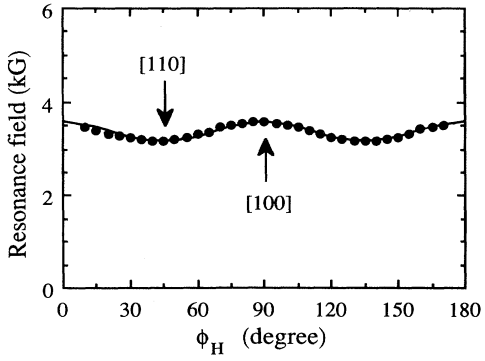

FIG. 2. The angular dependence ϕ_H of the in-plane FMR resonance field for the Ni (60 Å)-Cu(45 Å) film (No. 3). The solid line corresponds to the fit using the parameters in Table I.

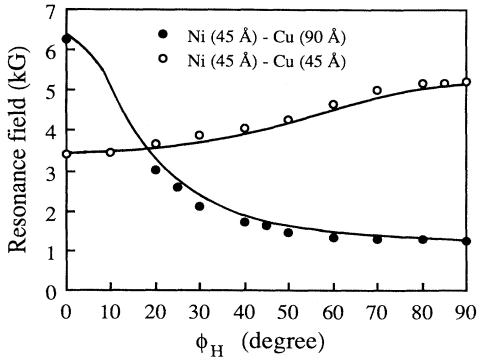

FIG. 3. The angular dependence ϕ_H of the out-of-plane FMR resonance field for the Ni (45 Å)-Cu(45 Å) film (No. 2) and the Ni (45 Å)-Cu(90 Å) film (No. 6). The solid lines correspond to the fit using the parameters in Table I.

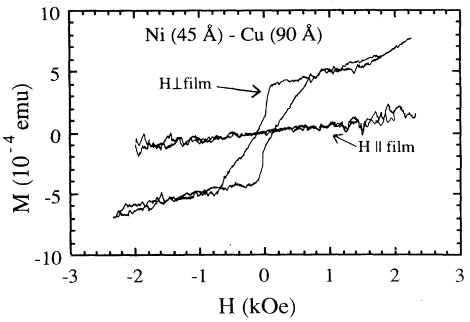

FIG. 4. The magnetization curve of Ni (45 Å)-Cu(90 Å) film (No. 6) for magnetic fields applied perpendicular and parallel to the plane of the film.

perpendicular anisotropy. This is further demonstrated in Table I for other films. The effect of the Cu layer thickness (30–120 Å) for a fixed Ni layer thickness (45 Å) upon the strain modulations is clearly seen in the differing values of $(\varepsilon_\perp - \varepsilon_\parallel)$ for Ni in these superlattices. Even though the distortion $(\varepsilon_\perp - \varepsilon_\parallel)$ for the Ni lattice is about 50% greater for thicker Cu layer films, there is less strain on the Cu lattice as its lattice spacing approaches that of bulk. We suspect that the strains in the thicker Cu layer film are relieved by misfit dislocations. Overall there appears to be a direct correspondence between the strain and the perpendicular uniaxial anisotropy as increasing values of the distortion $(\varepsilon_\perp - \varepsilon_\parallel)$ result in larger values of H_u.

In order to determine the effect of the magnetostriction on the perpendicular magnetic anisotropy, a strain-induced magnetic anisotropy field is calculated according to the following expression:[15]

$$H_u = (3/M_s)\lambda_{100}(C_{11} - C_{12})(\varepsilon_\perp - \varepsilon_\parallel) . \quad (1)$$

λ_{100} is the linear magnetostriction constant along $\langle 100 \rangle$ direction and C_{11} and C_{12} are the cubic elastic constants. For bulk Ni, $M_s = 485$ emu/cm^3, $\lambda_{100} = -45.9 \times 10^{-6}$, $C_{11} = 2.5 \times 10^{12}$ dynes/cm^2, and $C_{12} = 1.6 \times 10^{12}$ dynes/cm^2. Utilizing the measured strains, the calculated values of H_u are comparable to the experimentally determined values as shown in Table I. For films (Nos. 2, 3, 4, and 9) with the easy axis in the plane of the film, the calculated H_u values exceed the experimental values by less than 15%; while for remaining films, the values are within 6%. The quantitative agreement between the calculated and experimentally determined values of H_u suggests that the strain-induced magnetic anisotropy due to the inverse magnetostriction could be responsible for the uniaxial perpendicular anisotropies. Nevertheless, earlier work attributed the positive uniaxial anisotropy mainly to the interface-induced anisotropy[7] which is inversely proportional to the thickness of the magnetic layers. Plots of H_u versus 1/Ni thickness for constant Cu layer thicknesses of 45 and 90 Å result in linear fits with nonzero intercepts of 1.7 and 5.0 kG, respectively, in the infinite thickness limit. Although the 1/thickness behavior is in qualitative agreement with the interface-induced anisotropy mechanism, the large nonzero H_u values in the infinite-thickness limit indicate that the induced magnetic anisotropy is distributed throughout the entire film, not just at the interface, and that an alternate source for the magnetic anisotropy must be present to account for the large H_u values. As shown in an earlier study,[16] thick (≥ 50 Å) Ni films remain more heavily strained than expected from theory. Consequently, the strain-induced magnetic anisotropy arising from the inverse magnetostriction of the Ni seems to be mainly responsible for the observed uniaxial perpendicular anisotropies in these superlattices.

We have also observed another interesting feature in the FMR scans on film No. 2 for the perpendicular orientation (applied magnetic field perpendicular to the plane of the film). In addition to the main resonance field of 5.2 kG at $\phi_H = 90°$, a second weaker resonance is observed at a lower field of ≈ 3.5 kG. This second resonance may be associated with a slightly larger strain arising from the growth of the first Ni layer on the bulklike Cu(100) seed layer. The remaining Ni layers in the superlattice may be strained less because of the intervening strained Cu layers and give rise to the main resonance field. The observation of this second resonance peak indicates the utility of the FMR technique to distinguish several interfacial effects in multilayer magnetic films.

In summary, we have found that magnetostriction plays a significant role on the magnetic anisotropy of multilayer magnetic films. By combining structural (XRD) and magnetic (FMR) techniques to characterize $\langle 100 \rangle$-oriented Ni-Cu superlattices, the uniaxial perpendicular and magnetocrystalline anisotropies have been determined as function of thickness and strain in the Ni and Cu layers. Utilizing the measured strain with known elastic and magnetostriction constants for bulk Ni, the calculated strain-induced magnetoelastic anisotropies due to an inverse magnetostriction are found to be in good quantitative agreement with the uniaxial perpendicular anisotropies experimentally determined for these superlattices and correspondingly the main cause for these anisotropies. Furthermore the strain in Ni layers in these superlattices can be increased sufficiently with increasing Cu thickness so as to change the direction of the easy magnetization axis.

The authors wish to thank Professor G. L. Dunifer for providing access to the 12-GHz FMR spectrometer. This research was supported by the National Science Foundation, Grant No. DMR-9321127.

[1]Z. Zhang, P. E. Wigen, and S. S. P. Parkin, J. Appl. Phys. **69**, 5649 (1991).

[2]C. H. Lee, R. F. C. Farrow, C. J. Lin, E. E. Marinaro, and C. J. Chien, Phys. Rev. B **42**, 11 384 (1990).

[3]F. J. A. den Broeder, W. Hoving, and P. J. H. Bloemen, J. Magn. Magn. Mater. **93**, 562 (1991); F. J. A. den Broeder, D. Kuiper, H. C. Donkersloot, and W. Hoving, Appl. Phys. A **49**, 507 (1989); H. J. G. Draaisma, W. J. M. de Jonge, and F.

J. A. den Broeder, J. Magn. Magn. Mater. **66**, 351 (1987).
[4]B. N. Engel, C. D. England, R. A. Leeuwen, M. Nakada, and C. M. Falco, J. Appl. Phys. **69**, 5643 (1991); B. N. Engel, C. D. England, R. A. Leeuwen, M. H. Wiemann, and C. M. Falco, *ibid.* **70**, 5873 (1991); Phys. Rev. Lett. **67**, 1910 (1991).
[5]F. J. A. den Broeder, D. Kuiper, A. P. van de Mosselaer, and W. Hoving, Phys. Rev. Lett. **60**, 2769 (1988).
[6]C. H. Lee, Hui He, F. J. Lamelas, W. Vavra, C. Uher, and Roy Clarke, Phys. Rev. B **42**, 1066 (1990); Phys. Rev. Lett. **62**, 653 (1989).
[7]L. Néel, J. Phys. Radiat. **15**, 376 (1954).
[8]P. Bruno and J. P. Renard, Appl. Phys. A **49**, 499 (1989); P. Bruno, J. Appl. Phys. **64**, 3153 (1988).
[9]For a review on this subject, see B. Heinrich and J. F. Cochran, Adv. Phys. **42**, 523 (1993).
[10]Chin-An Chang, Appl. Phys. Lett. **57**, 297 (1990); J. Appl. Phys. **68**, 4873 (1990).
[11]G. Bochi, C. A. Ballentine, H. E. Inglefield, S. S. Bogomolov, C. V. Thomson, and R. C. O'Handley, in *Magnetic Ultrathin Films: Multilayers and Surfaces / Interfaces and Characterization,* edited by B. T. Jonker, S. A. Chambers, R. F. C. Farrow, C. Chappert, R. Clarke, W. J. M. de Jonge, T. Egami, P. Grünberg, K. M. Krishnan, E. E. Marinero, C. Rau, and S. Tsunashima, MRS Symposia Proceedings No. 313 (Materials Research Society, Pittsburg, 1993), p. 309.
[12]R. Naik, C. Kota, J. S. Payson, and G. L. Dunifer, Phys. Rev. B **48**, 1008 (1993).
[13]B. Demczyk, R. Naik, G. W. Auner, C. Kota, and U. Rao, J. Appl. Phys. **75**, 1956 (1994).
[14]F. J. Lamelas, H. David He, and Roy Clarke, Phys. Rev. B **43**, 12 296 (1991).
[15]S. Chikazumi and S. H. Charap, *Physics of Magnetism* (Wiley, New York, 1964).
[16]J. W. Matthews and J. L. Crawford, Thin Solid Films **5**, 187 (1970).